On Commutation Modeling in Bond Graphs

Sergio Junco, Gonzalo Diéguez, Facundo Ramírez

Departamento de Electrónica
Facultad de Ciencias Exactas, Ingeniería y Agrimensura
Universidad Nacional de Rosario
Ríobamba 245 Bis – S2000EKE Rosario – Argentina

sjunco@fceia.unr.edu.ar, gdieguez@fceia.unr.edu.ar, facuram@citynet.net.ar

Keywords: Switched Bond Graphs, Switched Power Junctions.

Abstract: This paper revisits the Switched Power Junction or SPJ-formalism and shows that a SPJ can be represented by a suitable combination of standard BG-junctions and boolean modulated transformers (*b*MTF). This allows for an easy implementation of SPJs in BG-oriented simulation software, as it is shown via its programming in *20sim*®. Modeling and simulation of the following applications are presented: a three-phase inverter with an RL-load; a series DC-motor with its field inductance varying causality due to a switch provided for field-weakening; and a ¼-car model with a dissipator changing causality due to the car jumping and leaving the ground. These examples illustrate that the combination of SPJs and *b*MTFs (hence, of standard BG-junctions and *b*MTFs, in essence) is able to overcome the insufficiency of other methods associated to varying causality in switches and/or regular, "continuous" BG-components.

1. INTRODUCTION

In many engineering problems abrupt changes in physical systems are considered to occur instantaneously. This is mainly due to the facts that the behavior the engineer is interested in has a time scale much bigger than that of the abrupt change, and that the details inside the time window of this change are not relevant to the behavior under study. Thus, ignoring them results in saving analysis and simulation time and effort. However, this assumption requires a special treatment as modeling discontinuous behavior may possibly involve many facets like changing model structure and variables, instantaneous jumps in state values of otherwise continuous variables, etc., see [1] for detailed discussion of some of these issues.

The need to incorporate some tools to handle these problems has been recognized by the Bond Graph (BG) research community. Indeed, being a physically oriented formalism, BG-theory has been originally conceived to handle only continuous phenomena. Many ideas and techniques have been proposed to treat idealized commutations. The most relevant among them are: boolean-modulated transformers *b*MTF [2]; switching bonds, commanded by a finite-state automaton [3]; the ideal switch Sw, enforcing zero effort or zero flow on a suitably chosen junction [4], [5]; the controlled junction mechanism, which can assume two states, on (where it behaves like a normal BG-junction) and off (where it disconnects all the components attached to the junction) [1],[6]; the concept of commutation cells [7], [8], introduced to deduce a unique state equation with variable parameters when causality changes only occur on switches or resistive components; the switched power junction, SPJ, which is a 0- (or 1-)junction that admits more than one effort- (flow-) deciding bond, with the constraint that one and only one of these bonds is active at a given time instant [9]. Some of these formalisms have been proposed as alternatives to others among them in order to circumvent some associated modeling drawbacks like varying causality of switching-modeling components, hanging junctions, failure to disconnect subsystems, and other inconsistencies. Also switched inertias and capacitors have been suggested [10], as well as addition of parasitic phenomena to the ideal switching components, like (possibly nonlinear) resistors, and sometimes also capacitors. See [9], [11] for an assessment of these issues.

This paper exclusively addresses the BG-representation of model commutation with ideal switching components (no power consumption). Particularly it will focus on the *b*MTF- and SPJ-formalisms. This is done beginning in the next section, which shows that the SPJs originally introduced in [9] in a compact form can be synthesized each in an expanded form using two standard BG-junctions and a suitable number of *b*MTFs. In Section 3, both, compact and expanded *20sim*® [12] implementations of SPJs are presented. In Section 4 some modeling and simulation examples that use SPJs and *b*MTFs are addressed. The problem of varying causality when switching between system configurations is shown to be simultaneously solved. The simulation results confirm the correctness of the models. Section 5 presents the conclusions.

2. STANDARD JUNCTIONS, BOOLEAN MODULATED TRANSFORMERS AND SWITCHED POWER JUNCTIONS

2.1 Definition of Switched Power Junctions

Switched Power Junctions have been introduced in [9] as a generalization or extension of standard BG-junctions. Fig. 1a,b depicts a 0- and a 1-junction, respectively, including a possible, admissible causality assignment to the adjacent bonds [2], [13]. Note that one and only one causal stroke can be on the 0-junction side, and all but one causal strokes must be on the 1-junction side. As it is well known, Eqs. (1) and (2) correspond to these configurations.

For the 0-junction

$$\begin{aligned} e_i &= e_1 \quad ; \quad i = 2,\dots,n+2 \\ f_1 &= f_{n+1} + f_{n+2} - f_2 - \cdots - f_n \end{aligned} \tag{1}$$

For the 1-junction

$$\begin{aligned} f_i &= f_1 \quad ; \quad i = 2,\dots,n+2 \\ e_1 &= e_{n+1} + e_{n+2} - e_2 - \cdots - e_n \end{aligned} \tag{2}$$

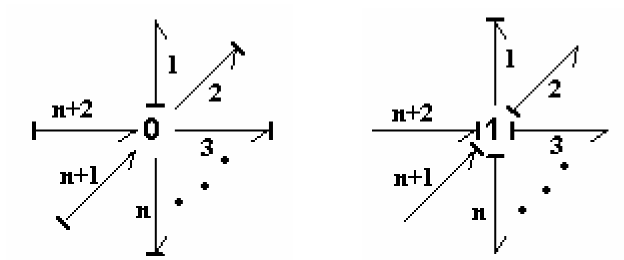

(a) (b)

Fig. 1. Standard 0- and 1-junctions with causality assignment.

The generalized models of both 0_S and 1_S (the notation for 0- and 1-switched power junctions, respectively) are shown in Fig. 2 as they have been introduced in [9]. If they were standard junctions there would be a causal conflict in each of both cases. In the new formalism the causal conflict is removed via imposing the constraint that one and only one of the effort-(flow-)deciding bonds imposes the effort (flow) to the 0_S (1_S) at any given time instant. This convention is graphically represented by the presence of the activated bond in the junction symbol, and mathematically formalized in (3) and (4) for the 0_S and 1_S, respectively. Only one of the boolean variables in the set $\{U_1, U_2, U_3, \dots, U_n\}$ is allowed to have the value 1 at a given time instant, the rest are zero. Looking at (3) and (4) it is seen that the boolean variables assuming the zero values annihilate both effort and flow in each of the associated bonds, and thus completely disconnect all subsystems at the bond-ends opposite to the junction.

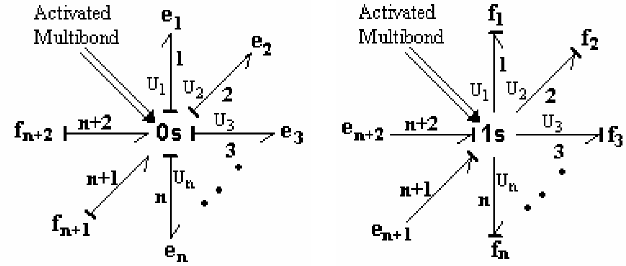

Fig. 2. Generalized 0_S- and 1_S-junctions. Original, compact notation.

$$\begin{aligned} &\textit{Junction effort} = U_1 e_1 + U_2 e_2 + \cdots + U_n e_n \\ &f_i = U_i\left(f_{n+1} + f_{n+2}\right) \quad ; \quad i = 1,\dots,n \end{aligned} \tag{3}$$

$$\begin{aligned} &\textit{Junction flow} = U_1 f_1 + U_2 f_2 + \cdots + U_n f_n \\ &e_i = U_i\left(e_{n+1} + e_{n+2}\right) \quad ; \quad i = 1,\dots,n \end{aligned} \tag{4}$$

2.2 Expanded Representation of SPJs

While representing 0_S- and 1_S-junctions as in Fig. 2 is a good, worth-keeping compact notation, it is useful to show that these junctions can be obtained using a combination of standard BG-junctions and boolean MTFs with the variables U_i as moduli. Let's explain how it works in the case of the 0_S-junction.

Expanded 0_S-Junction

Define the "*0_S-Junction Effort*" (noted e_{0s}) and the "*0_S-Junction Flow*" (noted f_{0s}) as in (5) and (6), respectively. The first of these equations can be represented with the structure in Fig.3b, which uses a standard 1-junction and *b*MTFs, while the second is captured in Fig. 3a by a structure with a standard 0-junction.

$$e_{0_S} \mathrel{\hat{=}} U_1\, e_1 + U_2\, e_2 + \dots + U_n\, e_n \tag{5}$$

$$f_{0_S} \mathrel{\hat{=}} f_{n+1} + f_{n+2} \tag{6}$$

Now, looking at the first line of (3) it is realized that the e_{0s} is imposed onto bonds #(n+1) and #(n+2), i.e., the undetermined effort (e = ???) in Fig. 3a is just $e = e_{0s}$. At the same time, looking at the remaining lines in (3), it is seen that the f_{0s} is imposed to the bonds #1' to #n', i.e., the undetermined flow (f = ???) in Fig. 3b is just $f = f_{0s}$. The observed complementarity suggests fusioning the structures of Figs.3a and 3b into a unique structure sharing a bond with the newly defined e_{0s} and f_{0s}.

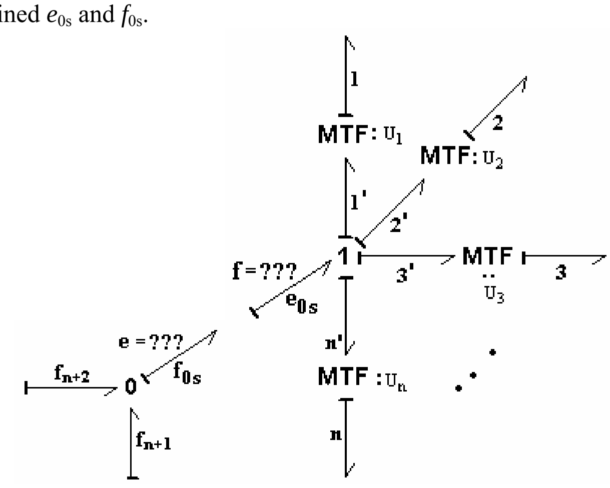

(a) (b)

Fig. 3. Analyzing the 0_S-Junction.

The equivalence of this detailed structure with the 0_S-junction is highlighted in Fig. 4. Observe that in the expanded representation there is no need to invoke any condition on the variables $\{U_1, U_2, U_3, \ldots, U_n\}$ in order to prevent a causal collision. Indeed, whatever the moduli U_i are, there is no causal conflict at all. This fact is due to the presence of the standard 1-Junction in the structure.

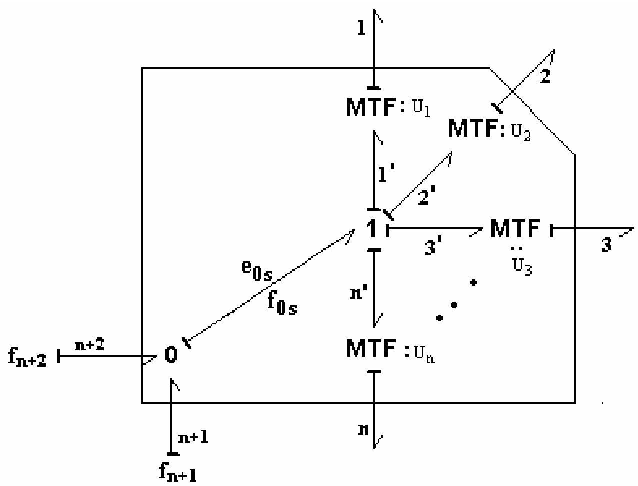

Fig. 4. Expanded representation of the 0_S-Junction.

Expanded 1_S-Junction

An analysis similar to the previous one yields the expanded representation of Fig. 5 for the 1_S-Junction.

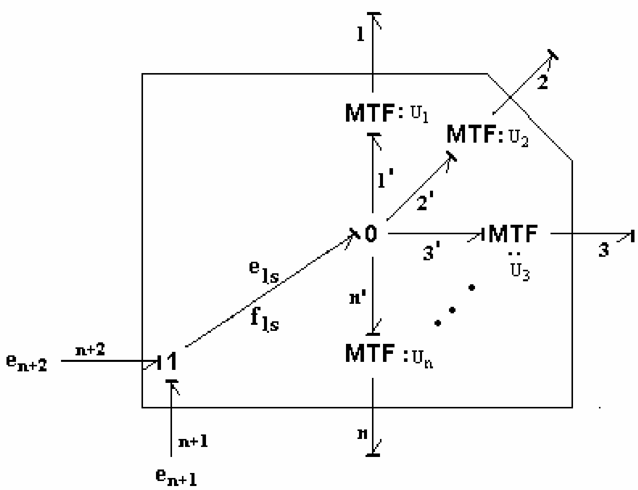

Fig. 5. Expanded representation of the 1_S-Junction.

3. *20SIM* IMPLEMENTATION OF SPJs

This section presents the implementation on *20sim*® of both, the compact and the expanded representations of the SPJs. *20sim*® is a “dynamic modeling and simulation program for iconic diagram, bond graph, block diagram and equation models” [12]. Its main components are the *20sim* Editor and the *20sim* Simulator. Fig. 6a shows part of an Editor screen where a 1- and a 0-junctions can be seen. The subwindow “Type” specifies the interconnection ports of the selected 0-junction, which can have any number *p* of power ports (black box means incoming power positive), and one outgoing (white box) signal representing the unique junction-effort. At one level of representation deeper one can see the four *20sim*-code lines implementing the 0-junction as shown in Fig. 6b. Three lines are declared as equations: the first line specifies that the sum of the (after the power harpoons in the graphical representation) directed flows equals zero; the second tells that all efforts are equal; the third specifies the port imposing the common effort.

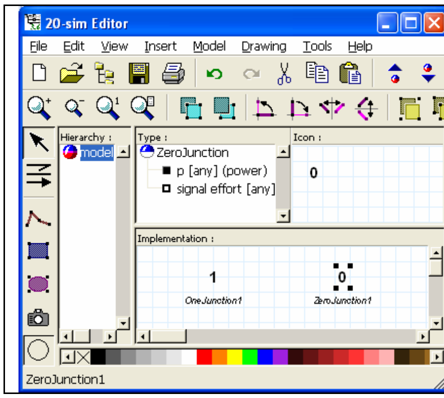

Zero-Junction Implementation:

equations
sum (*direct* (p.f))=0;
equal (*collect* (p.e));
effort = *first* (p.e);

(a) (b)

Fig. 6. (a) *20sim* Editor Screen, with 0- and 1-Junction. (b) Implementation of standard 0-Junction.

Compact 0_S-Junction

The implementation of the compact 0_S-Junction will be explained with the help of Figs. 7 and 8 and the code in Table 1. The editor screen shows that this particular 0_S-Junction has been endowed with three power ports (two of them with ingoing positive power-flow, the third with outgoing positive power flow) and with an ingoing signal port. This corresponds to the graphical representation in Fig. 8, where the bonds numeration is correlated with that of the junction-ports in Fig 7.

The first line of Table 1 declares a real variable defined some lines below as U_inv = (1-U), where U is the junction control variable (even though both take on only the values 1 and 0, they are defined as real because of software consistency issues). The boolean variables “up” and “down” declared in the sequel are not fundamental to the SPJ definition, but serve to force event driven simulation at the switching instants.

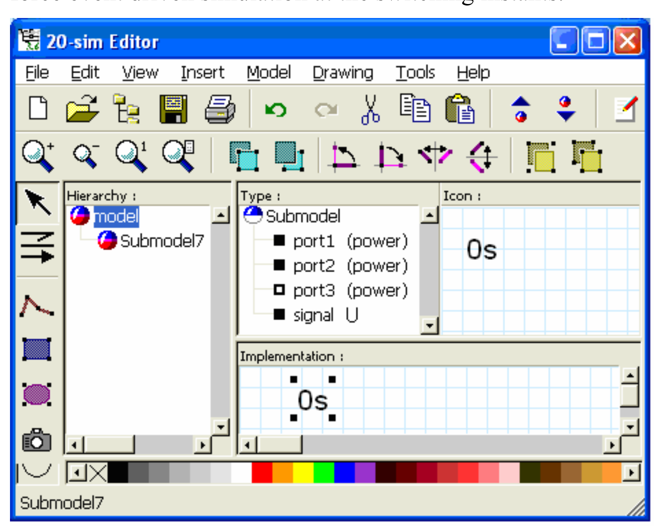

Fig. 7. *20sim* Editor Screen, with 0_S-Junction.

The events are generated some lines below using the *20sim* event-function (generates event when argument becomes zero). The “initialequations” facility of *20sim* have been found useful to avoid numerical inconsistencies at simulation start-up. The last block is the implementation of (3) in *20sim* code: the effort e_3 alternatively assumes the values of efforts e_2 and e_1 according to the value of the control variable “U”; dually, f_1 and f_2 switch complementarily between f_3 and zero, also driven by “U”. The compact implementation of a 1_S-Junction is fully similar.

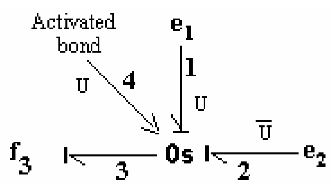

Fig. 8. The 0_S-Junction described in Table 1.

Table 1. Implementation of compact 0_S-Junction:

```
variables
        real U_inv;
        boolean up;
        boolean down;

initialequations
port3.e=0;

equations
        up = event(U – 1 );
        down = event(U);

        U_inv = (1 – U;

        port3.e = U*port1.e +U_inv*port2.e;
        port1.f = U*port3.f;
        port2.f = U_inv*port3.f;
```

Expanded 0_S-Junction

At the highest representation level the 0_S-Junction looks like the compact one in Fig. 7, but at one level deeper, instead of the *20sim*-code there is again a graphical representation which uses standard *20sim* BG components, see Fig. 9. Again in this case, the realization of a 1_S-Junction is similar.

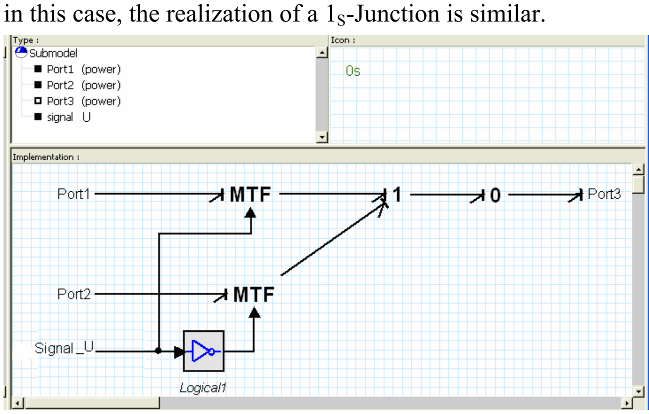

Fig. 9. *20sim* model of expanded 0_S-Junction.

Its functioning is self-explanatory knowing that the MTFs have complementary boolean moduli. All the programming the user needs to do is just coupling components already available in the *20sim* library.

4. MODELING AND SIMULATION EXAMPLES

Three technically relevant systems are modeled in this section. The three-phase inverter with RL-load first presented serves to illustrate a standard switching problem without any causality changes. The series DC-motor addressed next features varying causality in its field inductance when transitioning between the full-excitation and the field-weakening modes. Finally, the ¼-car model has a dissipator changing causality due to the car jumping and leaving the ground. See Appendix for the numerical data employed in the simulation experiments.

4.1 Three-phase inverter

The basic transistor inverter in Fig. 10 is modeled in Fig. 11 assuming that each transistor-diode pair behaves like an ideal switch, which results in complementary binary states for each converter half-bridge. The modeling with SPJs is explained in Fig. 12 on one of its three identical half-bridges or columns -that associated to the “a” inverter-output terminal. The 1_S-junctions model the switching of each diode-transistor pair current between the line current Ia (switch “on”) and zero (switch “off”). The 0_S-junction models the corresponding switching of the terminal voltage between the dc-link voltages +E and –E.

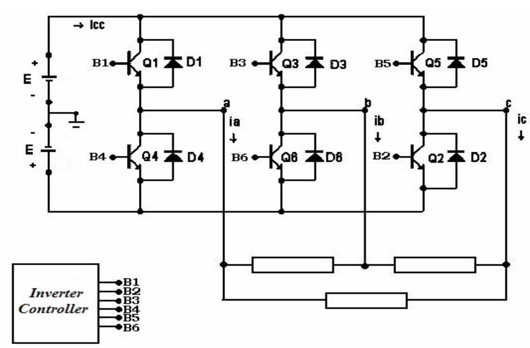

Fig. 10. Switched Three-Phase Transistor Inverter.

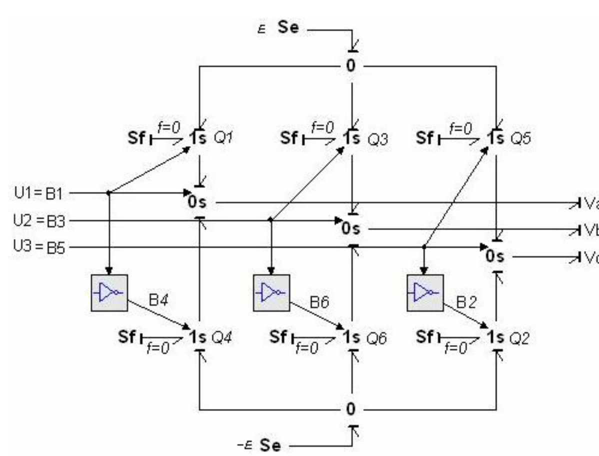

Fig. 11. SPJ BG-model of switched three-phase inverter.

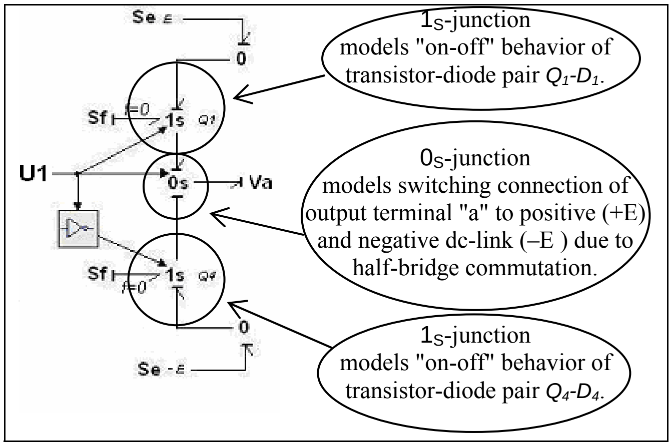

Fig. 12. SPJ-model of inverter half-brige.

The inverter model has been used to simulate the supply to a Δ-connected 3-phase RL-load with a six-step inverter modulation policy [14] providing the control signals U_i to the transistor bases B_i (cf. Figs. 10 and 11 for this notation).

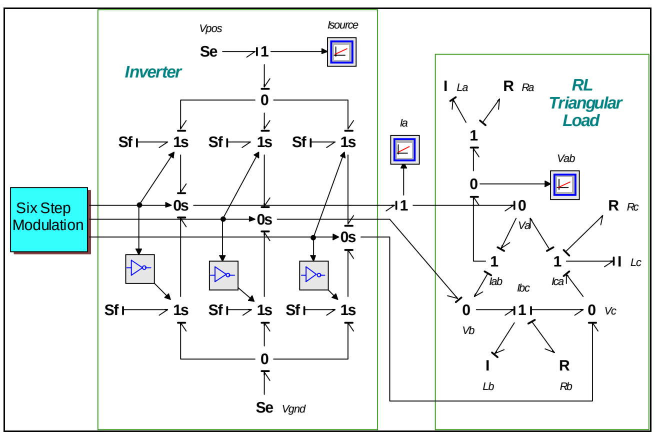

Fig.13. BG-model of inverter-supplied electrical system.

The few waveforms shown in Fig. 14 allow to appreciate the correctness of the results and the advantage of the object-oriented (OO) feature of BG-modeling.

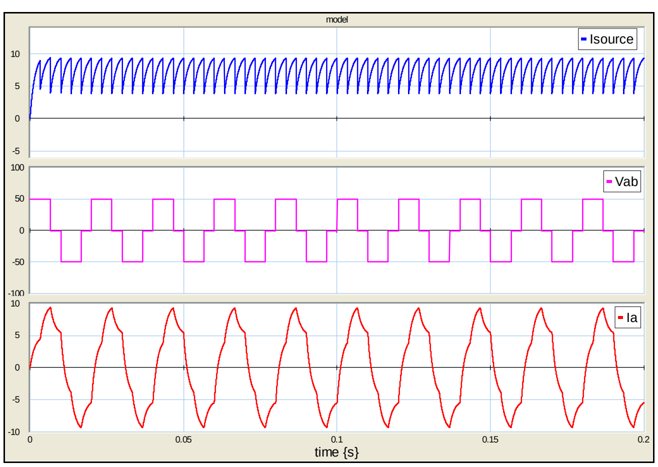

Fig.14. Simulated waveforms in inverter-supplied system.

The first plot is the dc-link current I_{CC} flowing through the constant supply inverter source. The piecewise constant function in the middle, assuming 3 levels, is the line-to-line voltage V_{ab}. The plot at the bottom is the line current Ia, a piecewise composition of first order exponential functions due to the stepwise inverter supply to the linear RL-load. It is clearly seen that, as all circuit component and variables are represented in the BG, any variable of interest can be observed at any moment.

4.2 Series DC-Motor

Consider the equivalent circuit of the electrical DC-Motor in Fig. 15, where the shunt, switched resistor R_d is provided in order to weaken the field excitation when the machine is run above base speed [15]. The switched BG of Fig. 16 shows that when the switch is "off" during operation at full excitation, the armature current is imposed (just a modeller choice) on the series RL nonlinear model of the field coil (dotted box on the right of the 0_S-junction is active). This results in derivative causality of the nonlinear field inertia, and the voltage drop across point 1 and 2 being calculated by the series subcircuit, as decided by the 0_S-junction control signal (a "0" goes through the relay on the right when motor speed is below base speed). When above base speed, the switch is "on" (a "1" goes through the relay) and the machine operates in the field-weakening region. The connection of the shunt resistor allows the field inertia to recover integral causality, so that the series subcircuit calculates current and the shunt resistor computes the voltage drop across 1 and 2. Thus, the box on the left of the 0_S-junction becomes active. Another relay is necessary to select the correct value of the excitation flux, corresponding to the field inertia model being active, in order to modulate the gyrator performing the electromechanical energy conversion.

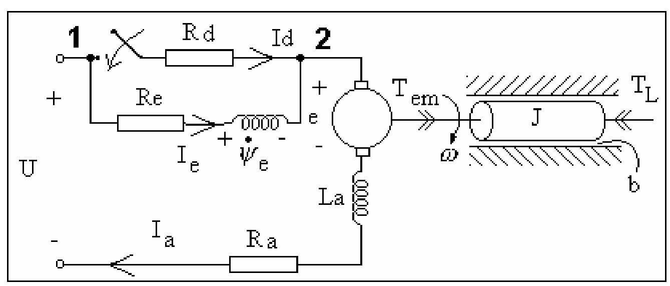

Fig.15. Series DC-Motor with field-weakening shunt resistor

As observed, there is a causality change in a system component (the nonlinear field inertia I_{NL}) due to the switching. Nothing can be done against, unless changing the modeling approach (for instance, leaving the OO-paradigm and lumping together both inertias being in series in the switch on-state) or its assumptions. Yet this is no problem, for the SPJ-formalism allows to represent all system modes in a unique BG.

The results of a most simple simulation experiment are shown in Fig. 16. The machine is supplied at $t = 0s$ with a ramp voltage saturating at $t = 1s$ and loaded at $t = 1.5s$ with a constant torque. In-between the rotor reaches the base speed, the switch commutates, and the armature and field currents depart from each other. Note that changing causality in I_{NL} demands initializing its state at the switching instant.

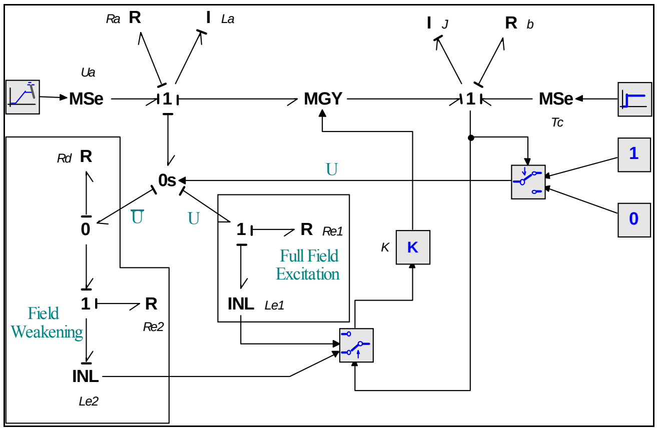

Fig.16. Switched BG-model of series DC-Motor.

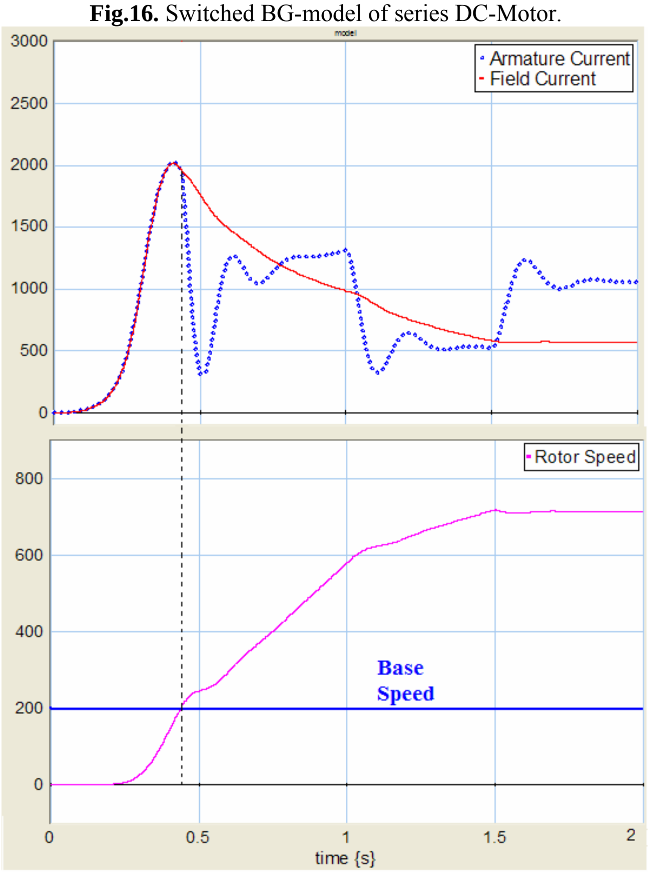

Fig.17. BG-model of inverter-supplied electrical system.

4.3 Jumping ¼-Car Model

A well-known ¼-car model is shown in Fig. 18. Loosing ground contact following a wheel impact with a road-bump is admitted and modeled in the switched BG of Fig. 19. Upward the regular 0-junction placed second from the top (where the normal force is recorded) the BG is a standard one. The switching is modeled below. When the tire looses ground contact, the damper-spring pair "d_t, k_t" gets disconnected from the rest of the system ($z_4 \neq z_3$). The switching conditions are: to decouple, the ground-tire normal force becoming zero; to reconnect, the tire getting again in contact with the road. The block "Control Signal" accordingly elaborates the switching command U (=1 ⇒ in contact). The 0_S-junction selects as force applied from below to the wheel inertia (the effort on the vertical bond above the 0_S-junction) an effort between two alternatives: that generated by the pair "d_t, k_t" (U=1), and the zero force imposed by the effort source on the left (U=0, no contact). Complementarily, the flow transmitted by the 0_S-junction to the pair "d_t, k_t" (bond on the right of the junction) switches between the relative speed (v_3-v_1) and zero. The damper of the pair "d_t, k_t" changes its causality from impedance (input flow = v_3-v_1 ; U=1) to admittance (input effort imposed by the spring; U=0). Correspondingly, the flow into the capacitor commutes between the relative speed (U=1) and the speed calculated by the resistor when in admittance causality. The capacitor itself does not change causality. All this is modeled by the 1_S-junction and the boolean MTF, and requires replicating the damper model, as shown in Fig. 19.

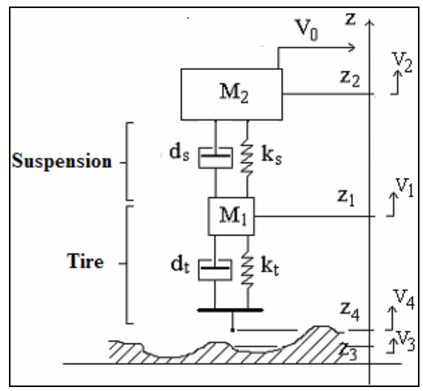

Fig.18. Ideal physical model of quarter-car.

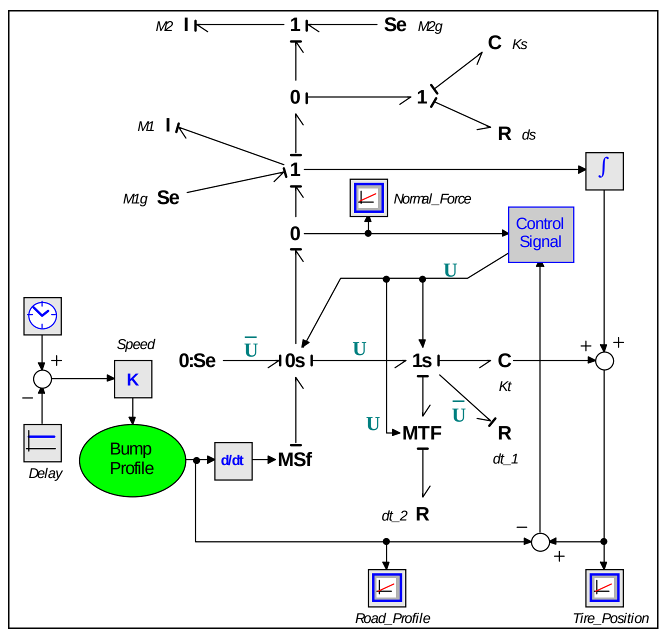

Fig.19. Switched BG-model of jumping quarter-car.

The plots in Fig. 20 illustrate the simulation results of the car being driven at 100 km/h over a 1m long and 10cm high bump. The common abcissa is the car horizontal position x.

The first plot shows the road profile (the bump) and the tire spatial trajectory $z_4(x)$. The second plot is the normal force and the two following are the events generated when the normal becomes zero and when the "flying car" reaches again the ground. Remark first the correspondance among the separation of the tire from the road profile, the annhilation of the normal force, and its hit crossing signal. Thereafter look at the correlation among the tire getting in contact with the road, the normal force deviating from cero and the hit crossing signal pertaining to this event.

The first plot shows that the tire position perfectly copies the road profile up to a certain point downhill the bump. What happens is that z_1 (evolution not shown) still increases after the bump crest while $z_4=z_3$ beginns to decrease, so that the damper relative speed becomes negative and its force starts compensating the force of the spring, which is still compressed. These forces subtract until the normal force becomes zero, and z_4 and z_3 go apart. Immediately thereafter the spring continues to expand until it dissipates its entire energy on the damper in a first order exponential process; this happens at the local minimum shown in the magnified view of the trajectory. Thereafter, there is no more dynamics in the pair "d_t, k_t" and z_4 simply copies the evolution of z_1 until the tire hits the road and the model switches again.

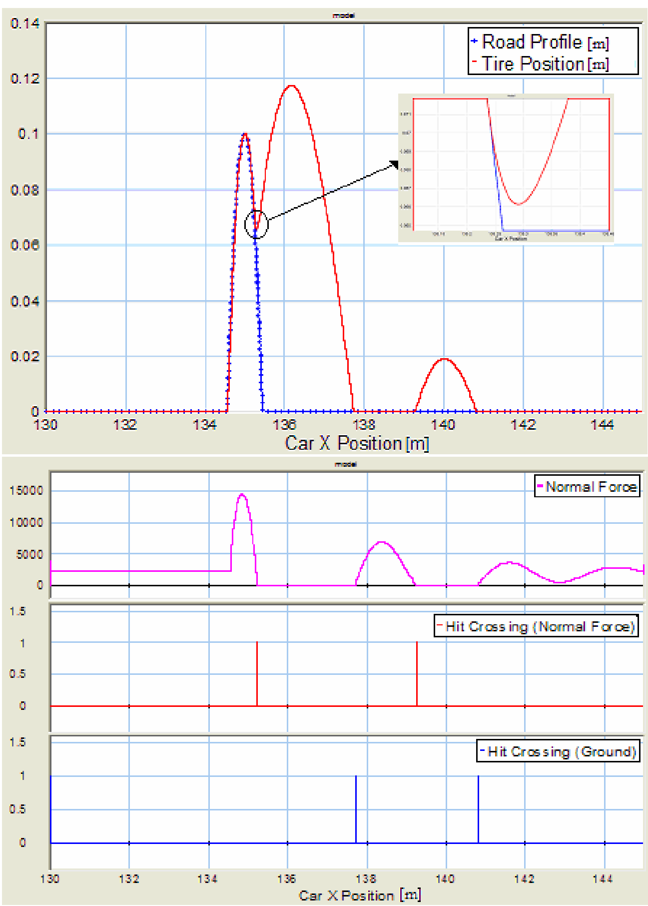

Fig.20. Switched BG-model of jumping quarter-car.

The subsequent behavior can be imagined as that of a (complex, horizontally sliding and vertically) bouncing ball, which is very well-known and exempts of further explanation.

5. CONCLUSIONS

This paper presented an analysis of the 0_S- and 1_S-SPJ-junctions and their ensuing expanded realizations with BG-standard 0- and 1-junctions and boolean MTFs. The software implementation on *20sim®* of both, the original and the expanded formulation of SPJs, have also been addressed. It has been shown that a unique causal BG with fixed causality can be formulated for systems with commutations just using the SPJs and boolean MTFs as ideally switching (no power consuming) BG-elements. This releases the modeler and simulationist of using parasitic non-ideal elements in the models, which are usually introduced to avoid causality problems at the possible price of having algebraic loops and stiff systems. A three-phase inverter, a series DC-Motor with a switched resistor, and a jumping ¼-car model, have been succesfully modeled and simulated in order to demonstrate the suitability and the properties of the proposed results.

REFERENCES

[1] P.J. Mosterman, G. Biswas, 1998, "A theory of discontinuities in physical systems models", *J. Franklin Institute*, 335B (3), pp. 401 - 439.

[2] Dean C. Karnopp, Ronald C. Rosenberg. 1992. *System dynamics–A Unified Approach*, 2nd ed., Wiley Interscience, Publications, New York.

[3] J. F. Broenink, K.C.J. Wijbrans, 1993. "Describing discontinuities in bond graphs". In: *Proc. ICBGM'93*, San Diego, CA, pp. 120-125

[4] J.E. Strömberg, J. Top, U. Söderman. 1993. "Variable causality in bond graph caused by discrete effects". In: *Proc. ICBGM'93*, San Diego, CA, pp. 115-119.

[5] Jan-Erik Strömberg. 1994. "A mode switching modelling philosophy", *Linköping Studies in Science and Technology*. Dissertations, No. 353, Linköping.

[6] P.J. Mosterman, G. Biswas, 1995. "Behaviour generation using model switching – A hybrid bond graph modelling technique". *Proc. ICBGM'95*, January, Las Vegas, pp. 177-182.

[7] Buisson J., Richard P.Y., Cormerais H., 2002, "Analysis of the bond graph model of hybrid physical systems with ideal switches", *Journal of Systems and Control Engineering*, Vol 216, Nº11, pp 47-72.

[8] Buisson J., Richard P.Y., Cormerais H., 2004. "Notion of Commutation Cells for the Modeling of Hybrid Systems using Ideal Switch Representation". In: *Proc. Int. Conf. on Integrated Modeling and Analysis in Applied Control and Automation* (*IMAACA'04*), Genoa, Italy, October 28-31, 2004, Vol. 2, pp. 21-28.

[9] A. C. Umarikar and L. Umanand. 2005, "Modelling of switching systems in bond graphs using the concept of switched power junctions", *Journal of The Franklin Institute*, 342, pp 131-147.

[10] P. J. Gawthrop, "Hybrid Bond Graphs Using Switched I and C Components", *CSC Report 97005*, University of Glasgow, July 10, 1997.
[11] G. Dauphin-Tanguy, C. Rombaut, 1993. "Why a Unique Causality in the Elementary Commutation Cell Bond Graph Model of Power Electronics Converter." In: *IEEE International Conference on SMC*, Le Touquet, 257-263.
[12] Controllab Products B.V., 20-sim™, http://www.20sim.com/product/20sim.html
[13] F. E. Cellier. 1991. *Continuous System Modeling*, Springer Verlag, New York.
[14] Holtz, J.(1994): "Pulse Width Modulation for Electronic Power Conversion", in *Proc. IEEE*, 82:8.
[15] Leonhard, W.: *Control of Electrical Drives*. 2nd Ed. Springer-Verlag, Berlin, 1997.
[16] Chiasson, J. (1994). "Nonlinear Differential-Geometric Techniques for Control of a Series DC Motor", *IEEE Trans. on Control Systems Technology* **2**, No. 1, 35-42.

APPENDIX: DATA OF SIMULATION EXAMPLES

Three-Phase Inverter

RL-load: R=10Ω, L=15mH.
DC-link: ±E = ±25V.
Switching Frequency (six-step fundamental): 50Hz.

Series DC-Motor

Source: [16]
U_{MAX} = 1000 V; $I_{a,MAX}$ = 1000 A.
ω_{MAX} = 6860 rpm; Base Speed, ω_B = 1910 rpm.
R_a = 9.89 mΩ; L_a = 1.4 mH; R_e = 14,85 mΩ; R_d = 16,96 mΩ.
K = 0.04329 Nm/WbA; J = 3 Kgm^2.
Maximum Load Torque beyond Base Speed, T_{MAX} = 1370 Nm.
Magnetization curve of excitation coil, ψ_e vs. I_e:

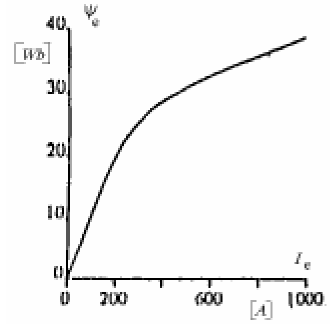

Quarter Car Model

Data from a Renault Clio RL 1.1
Vehicle weight, $4M_2$ = 8100N.
Tires, type and dimensions, 145 70 R13 S.
Maximum speed, $V_{0,MAX}$ = 146 Km/h.
Tire vertical stiffness, k_t = 150000 N/m.
Tire damping constant, d_t = 300 Ns/m.
Unsprung mass (at each wheel), M_1 = 38.42 Kg.
Suspension stiffness, k_S = 14900 N/m.
Damper coefficient, d_S = 475 Ns/m.